

## A SURF-Based Rigid Feature Tracking (RiFT) Approach for Cost-Effective Analysis of Fracture Behaviour in Asphalt Pavements

Yavuz ABUT\*

*Department of Transportation Engineering, Faculty of Engineering, Yalova University, Yalova, Türkiye*

*Received: 25.11.2025, Accepted: 19.12.2025, Published: 29.12.2025*

### ABSTRACT

Cracking in asphalt pavements significantly affects durability and service life, making accurate characterization of fracture essential. The Semi-Circular Bending (SCB) test is widely used to evaluate fracture resistance; however, conventional optical techniques such as Digital Image Correlation (DIC) require high-resolution cameras, controlled lighting, and speckle, leading to high costs and complex setups. This study introduces Rigid Feature Tracking (RiFT), a SURF-inspired (Speeded-Up Robust Features), feature-based displacement estimation framework designed for quasi-rigid materials under controlled loading. RiFT is specifically introduced to provide a robust, low-cost optical method for monitoring crack initiation and propagation during SCB test, overcoming the hardware and sample preparation limitations of DIC in this critical application. RiFT departs from correlation-heavy approaches by detecting sparse but robust landmark points and reconstructing dense displacement fields through edge-preserving interpolation, aim to reduce sensitivity to angular and illumination variations. SCB tests were performed on asphalt specimens with an INSTRON 5982, recording load and CMOD at 10 Hz. Images were captured every five seconds using a webcam without additional lighting or surface speckle. This study presents RiFT primarily as a methodological framework validated through controlled SCB experiments, demonstrating its proof-of-concept capability for real-time tracking, with further wide-scale validation planned for future work.

**Keywords:** Asphalt crack analysis; Digital image correlation; Semi-circular bending test; RiFT; SURF.

## Asfalt Kaplamalarda Kırılma Davranışının Maliyet Etkin Analizi için SURF Tabanlı Rijit Özellik Takibi (RiFT) Yaklaşımı

### ÖZ

Asfalt kaplamalarda çatlak oluşumu, dayanıklılığı ve hizmet ömrünü ciddi şekilde etkilemektedir. Bu nedenle kırılmanın doğru biçimde analiz edilmesi kritik öneme sahiptir. Yarı Dairesel Eğilme (SCB) testi, kırılma direncini değerlendirmek için yaygın olarak kullanılmaktadır. Ancak, Dijital Görüntü Korelasyonu (DIC) gibi optik yöntemler; yüksek çözünürlüklü kameralar, kontrollü aydınlatma ve benekler gerektirdiğinden maliyet ve karmaşık kurulum sorunları doğurmaktadır. Bu çalışmada, yarı-rijit malzemeler için tasarlanmış, SURF (Speeded-Up Robust Features) algoritmasından esinlenen ve özellik tabanlı yer değiştirme tahmin yöntemi olan Rijit Özellik Takibi (RiFT) sunulmaktadır. RiFT, bu kritik uygulamada DIC'nin donanım ve numune hazırlama kısıtlarını bertaraf ederek, SCB testi sırasında çatlak başlangıcını ve ilerlemesini izlemek için sağlam, düşük maliyetli bir optik yöntem sağlamak amacıyla özel olarak sunulmuştur. RiFT, korelasyon ağırlıklı yaklaşımlardan farklı olarak, seyrek güvenilir nirengi noktaları belirlemekte, kenar koruyucu enterpolasyonla yer değiştirme alanlarını yeniden oluşturarak,

farklı aç ve ışık değişimlerine duyarlılığı azaltmayı hedeflemektedir. SCB testleri, INSTRON 5982 cihazı kullanılarak asfalt numuneleri üzerinde gerçekleştirilmiş; yük ve CMOD 10 Hz'de kaydedilmiştir. Görüntüler, ek aydınlatma veya yüzey benekleri olmadan, her beş saniyede bir web kamerasıyla alınmıştır. Bu çalışma, RiFT'i öncelikle kontrollü SCB deneyleriyle doğrulanmış metodolojik bir çerçeve olarak sunmakta ve RiFT'in gerçek zamanlı izleme yapabildiğinin kavramsal ispatını ortaya koymaktadır. Daha kapsamlı doğrulama ise gelecek çalışmalar için planlanmaktadır.

**Anahtar Kelimeler:** Asfalt çatlak analizi; Dijital görüntü korelasyonu; Yarı dairesel eğilme testi; RiFT; SURF.

## 1. INTRODUCTION

Cracking in asphalt concrete is one of the most critical issues in pavement design and maintenance, as it directly affects the durability, service life, and overall performance of road infrastructure. Asphalt pavements are subjected to complex loading and environmental conditions, which lead to progressive damage over time. Among the various forms of distress, cracking is particularly detrimental because it accelerates moisture infiltration, weakens structural integrity, and increases maintenance costs ([Min et al., 2025](#)). Understanding the mechanisms of crack initiation and propagation is therefore essential for designing resilient pavements and optimizing mixture compositions ([Saha & Biligiri, 2016](#)).

Cracking mechanisms in asphalt concrete are generally classified into fracture cracking and fatigue cracking, each requiring distinct evaluation methods. Fatigue cracking typically occurs under repeated traffic loading, where micro-cracks gradually accumulate and coalesce into visible cracks ([Alsheyab et al., 2024](#)). In contrast, fracture cracking is associated with sudden failure under monotonic loading or extreme thermal conditions ([Marasteanu et al., 2012](#)), and reflective cracking occurs when underlying joints or cracks in the base layers propagate upward through the asphalt surface due to differential movement and stress concentration ([Son, 2014](#)). Over the years, researchers have developed various experimental setups to characterize these behaviours. According to [Zhou et al. \(2016\)](#), extensive research has focused on experimental designs for field validation of laboratory tests to evaluate the cracking resistance of asphalt mixtures, and standards for fatigue and fracture characterization have evolved over time. For fatigue assessment, commonly used tests include the four-point bending test ([AASHTO, 2017](#); [ASTM, 2021](#)), the Texas overlay test ([Texas, 2025](#)), and the indirect tensile fatigue test ([AASHTO, 2014](#)). For fracture characterization, widely adopted methods comprise SCB test—typically performed at low ( $-30\text{ }^{\circ}\text{C}$  to  $0\text{ }^{\circ}\text{C}$ ) and intermediate ( $5\text{--}25\text{ }^{\circ}\text{C}$ ) temperatures ([AASHTO, 2020a, 2020b](#); [ASTM, 2016](#); [EN, 2010](#))—along with the indirect tensile test ([ASTM, 2017](#)) and the disk-shaped compact tension test ([ASTM, 2013](#)).

The SCB test has gained prominence for its simplicity, efficiency, and adaptability. Using cylindrical specimens, which are easier to prepare than slabs or beams, SCB enables multiple samples to be extracted from a single core—an advantage for laboratory studies and quality control where material availability and time are critical ([Lu et al., 2021](#)). Under Mode I loading, the SCB test generates dominant tensile stress at the specimen's bottom, effectively simulating pavement cracking under tensile conditions while enabling the determination of critical fracture parameters such as fracture toughness, stress intensity factor, stiffness, compliance, fracture energy, and the J-integral within the frameworks of LEFM (Linear Elastic Fracture Mechanics) and EPFM (Elastic Plastic Fracture Mechanics) ([Saha & Biligiri, 2015](#)).

While primarily used for monotonic loading ([Birgisson et al., 2008](#); [Li & Marasteanu, 2010](#); [Saha & Biligiri, 2015](#)), some studies have extended SCB to cyclic loading ([Hassan, 2013](#); [Huang et al., 2013](#)) for

fatigue analysis, complemented by numerical simulations that model crack propagation and stress distribution. Several standards govern SCB testing, including EN 12697-44:2010 ([EN, 2010](#)), AASHTO TP 105-13 ([AASHTO, 2020a](#)), ASTM D8044-16 ([ASTM, 2016](#)), and AASHTO TP 124-18 ([AASHTO, 2020b](#)). These differ in specimen dimensions, notch lengths, loading rates, and fracture indicators—such as fracture toughness, J-integral, or Flexibility Index—though most recommend a 150 mm diameter. Recent research suggests smaller diameters (e.g., 100 mm) may also yield reliable results, but further validation is needed to ensure repeatability and conversion between sizes ([Lu et al., 2021](#)).

While SCB is a robust and widely accepted fracture test, capturing detailed crack evolution and displacement fields during testing remains challenging. Conventional optical measurement techniques such as Digital Image Correlation (DIC) have been extensively used in experimental mechanics to quantify deformation and strain fields ([Jiang-san et al., 2022](#); [Zhao et al., 2017](#); [Zieliński et al., 2025](#)). These methods rely on correlation-based tracking of intensity patterns between successive frames, which works well for fluid-like or granular motions where displacements are relatively large and directional variability is significant ([Asswad et al., 2024](#); [Liang et al., 2020](#)). In such cases, deformation fields are characterized by small amplitudes, local coherence, and abrupt discontinuities associated with crack initiation and propagation. As a result, traditional DIC algorithms often suffer from unstable correlation peaks, excessive false matches, and sensitivity to minor variations in illumination or surface texture. These limitations are particularly pronounced when displacements fall below the pixel scale, making accurate tracking challenging without costly high-resolution imaging systems and elaborate lighting setups. Moreover, implementing DIC in SCB experiments typically requires high-speed cameras, specialized lighting, and extensive calibration procedures to ensure accuracy ([Birgisson et al., 2008](#); [Wang et al., 2020](#); [Zhao et al., 2017](#)). These requirements increase both the cost and complexity of the experimental setup, limiting the practicality of such methods for routine testing or field applications. Additionally, the large volume of image data generated during high-frequency acquisition imposes significant computational demands, making post-processing time-consuming and resource-intensive. These challenges highlight the need for alternative approaches that are cost-effective, robust to imaging conditions, and capable of capturing fine-scale displacement and crack evolution without relying on expensive hardware or complex calibration.

To address these challenges, this study introduces a feature-based displacement estimation framework, termed RiFT, which builds upon the principles of the SURF algorithm developed by [Bay et al. \(2006\)](#), adapting them to the kinematic characteristics of quasi-rigid solids. Unlike correlation-heavy approaches, RiFT focuses on detecting sparse yet highly reliable landmark points and subsequently reconstructing a dense displacement field through edge-preserving interpolation guided by neighbourhood consistency. This strategy minimizes the need for extensive outlier suppression and instead leverages the spatial

coherence inherent in solid deformation. By doing so, RiFT provides a robust and computationally efficient alternative that is less sensitive to angular variations and lighting inconsistencies, eliminating the dependency on expensive imaging hardware or complex calibration procedures. The proposed framework is validated through controlled SCB experiments, demonstrating its capability to capture sub-pixel displacements and crack evolution patterns that remain elusive to conventional DIC analyses.

Beyond its technical robustness, RiFT offers significant practical advantages. By relying on standard imaging devices such as webcams and avoiding the need for specialized lighting or high-speed acquisition systems, the method drastically reduces experimental costs and setup complexity. [Cabo et al. \(2019\)](#) proposed a hybrid SURF-DIC algorithm that uses image matching and cross-correlation to estimate local displacements with subpixel precision, offering a fast, low-cost, and practical solution suitable for industrial applications. Although the original study by [Cabo et al. \(2019\)](#) focused on estimating local displacements in general structural applications using a hybrid SURF-DIC algorithm, the same concept is highly relevant for asphalt pavement cracking analysis, where accurate displacement tracking around crack tips is critical for evaluating fracture behaviour under SCB and similar tests. Furthermore, its adaptability to varying image quality and minimal calibration requirements make it suitable for field applications where controlled laboratory conditions are not feasible. These attributes position RiFT as a scalable solution for structural health monitoring, pavement performance evaluation, and other engineering contexts where crack detection and displacement tracking are critical yet resource constraints limit the use of traditional optical measurement systems. The SCB test remains a cornerstone in asphalt fracture characterization, but its full potential can only be realized through accurate and efficient measurement of crack evolution. The proposed RiFT framework addresses key limitations of existing optical methods, offering a practical and reliable alternative that aligns with the growing demand for cost-effective and adaptable testing solutions in pavement engineering.

By making full-field deformation analysis accessible and affordable during the standard SCB procedure, RiFT enhances the test's potential as a cornerstone for reliable, routine fracture characterization.

## **2. DIC-BASED ANALYSIS OF ASPHALT MIXTURES WITH SCB TEST**

To provide a clear overview of existing research, Table 1 synthesizes DIC-based studies relevant to asphalt mixtures. It consolidates related work and organizes it across key dimensions such as test and DIC variants, imaging and surface preparation, primary outputs and metrics, as well as limitations and research opportunities, offering a comprehensive reference for understanding methodological trends and gaps in this field.

**Table 1:** Summary of DIC-based studies on asphalt mixtures and SCB testing.

Reference	Theme	DIC techniques	Camera, Surface Preparation	Key Outputs
<a href="#">Birgisson et al. (2008)</a>	Determination & prediction of crack patterns in HMA using DIC	Plane 2D DIC (least-squares matching of grey-value windows)	Basler AF101, 1300×1030 px, 5 fps; ~5×4 cm ROI; white base + black speckle	Full-field displacement/strain; crack initiation/propagation; agreement with gauges (RMS ≈ 0.034%)
<a href="#">Zhao et al. (2017)</a>	Heterogeneous fracture simulation under SCB (cohesive crack model)	DIC used for displacement tracking; numerical FE focus	Industrial camera 1626×1236, 14 fps; focal 25 mm; speckle not reported	Load–displacement curve; final crack path for comparison with simulation
<a href="#">Zhang et al. (2018)</a>	Crack growth rate of sulfur-extended asphalt (cyclic SCB + DIC)	2D DIC for crack length at selected intervals; CMOD–crack length polynomial	“DIC camera” (unspecified); speckled (white + black dots)	Crack length, tip strain, FPZ; Paris law coefficients via da/dN from CMOD–a correlation
<a href="#">Górszczyk et al. (2019)</a>	Application of DIC for road materials	2D DIC (Istra 4D); NCC/LSM facets	Single camera; images at load steps; multi-LED lighting; white + black speckle	Displacement/strain maps; material moduli; crack visualization; rigid-body motion removal
<a href="#">Wang et al. (2020)</a>	Polymer-modified asphalt before/after aging (SCB + DIC)	Stereo (3D) DIC (VIC-3D); ZNSSD + Newton–Raphson	Dual CCD 1624×1224 @10 Hz; matte black base + white speckle	Exx(t); indices DE and JE; three cracking stages identified
<a href="#">Liang et al. (2020)</a>	“Use of Digital Image Processing” for fracture evaluation	Digital Image Processing (Otsu + median filtering) for crack pixels	HD camera (unspecified); no speckle; offline frame extraction	Crack path/length/area; fracture energy; aggregate effects
<a href="#">Radeef et al. (2021)</a>	Cracking resistance under repeated loading using Digital Image analysis	DIC + ImageJ DIP (fractal dimension, density, tortuosity)	High-res video camera (no fps/res given); speckle applied	Full-field strain; localization zones; geometric crack metrics for modifiers
<a href="#">Pei et al. (2021)</a>	Basalt fiber diameter effects (SCB + Ncorr)	2D DIC (Ncorr/Matlab); Cauchy strain; real-time L via DIC	Sony digital camera (unspecified); natural surface; no extra lighting noted	Three stages; fibers reduce strain; 7 μm fibers delay initiation (~4 s)
<a href="#">Jiang-san et al. (2022)</a>	Warm-mixed rubber powder modified asphalt (fatigue SCB)	Stereo (3D) DIC (VIC-3D 8)	Dual CCD; blue light; 1 Hz; white base + black speckle	Local strain evolution at notch; three damage stages; strain-rate turning point → fatigue life
<a href="#">Cheng et al. (2022)</a>	Long-term service pavement (SCB + stereo DIC)	Stereo (3D) DIC (GOM Correlate)	Two industrial cams (48×2048 px sensor), capable of 80 fps; blue light; acquired at 1 Hz; speckle	Horizontal strain maps; crack-tip strain evolution; strain-based fatigue damage parameter; 3-stage damage
<a href="#">Kong et al. (2023)</a>	Fiber-reinforced emulsified asphalt (cold-recycled)	DIC (GOM Correlate 2019); likely stereo	Two 2 MP CCD (Sony ICX274), 5 fps; LED spots; black-on-white speckle	U,V; Exx,Eyy; dU/dt, dExx/dt; FPZ size (e.g., 19.3 mm vs 16.4 mm)
<a href="#">Ouyang et al. (2023)</a>	Cement bitumen emulsion mixture fracture via DIC	3D (stereo) DIC; mean global Exx as failure indicator	Two cameras; “light system”; surface prep not specified	3D displacement/strain; mean Exx peak as failure; plastic zone area vs cement dosage (optimum ≈2.6%)
<a href="#">Asswad et al. (2024)</a>	Two-Part DIC (2PDIC) for crack propagation	2PDIC splits subset across discontinuity; pseudo-strain thresholds (ε=0.005/0.05)	3840×2748 px CCD, 1 fps; thermal chamber (–5 °C, 10 °C); black base + white droplets	COD; true crack length (L <sub>crack</sub> ); cumulative damage length (L <sub>damage</sub> ); tortuosity; energy reduction 22–63% vs ligament length
<a href="#">Ma et al. (2024)</a>	Cyclic SCB protocol at intermediate temperature	Stereo DIC (VIC-3D); virtual extensometer for CMOD; quadratic CMOD–a mapping	Stereo cams 1920×1200, 1 Hz; lighting system; white + black speckle	exx; CMOD; crack length time-history; validation vs clip-on extensometer (≤0.1 mm error); Paris-law n & logA
<a href="#">Zieliński et al. (2025)</a>	SCB + DIC for fracture properties (CivEng Vision)	2D DIC (ZNCC; sub-pixel interpolation)	DSLR Nikon D5300 (24 MP); intervalometer; strong LED (4000–5700 K); no speckle reported	Displacement maps; Exx,Eyy,Exy; crack path from initiation to failure; heterogeneity effects (REF vs RAS; aging)

To critically examine the data summarized in Table 1, several recurring technical and practical constraints in DIC applications for asphalt mixtures become evident. Early works such as [Birgisson et al. \(2008\)](#) and [Górszczyk et al. \(2019\)](#) demonstrated the ability of 2D DIC to provide full-field strain maps and visualize crack initiation, outperforming traditional point sensors. However, these setups relied heavily on painted speckle patterns and controlled lighting, which increases preparation time and cost. Similar requirements appear in [Jiang-san et al. \(2022\)](#), [Ma et al. \(2024\)](#), and [Zhang et al. \(2018\)](#) where white-and-black speckle patterns and LED or blue light sources were essential for correlation accuracy. This dependency limits field applicability and introduces variability when surface preparation is inconsistent. Another major limitation is temporal resolution. Many studies, including [Zhang et al. \(2018\)](#), [Jiang-san et al. \(2022\)](#), ([Cheng et al., 2022](#)), and ([Ma et al., 2024](#)), captured images at 1 Hz or selected intervals, making it difficult to track rapid crack propagation or micro-displacement events. Even when high-speed cameras were available ([Cheng et al., 2022](#); [Wang et al., 2020](#)), acquisition was often down-sampled to low frequencies for data management, sacrificing detail. This constraint is critical because SCB fracture involves sudden transitions that require finer temporal granularity. A third recurring issue is dimensionality and robustness near discontinuities. Most works ([Birgisson et al., 2008](#); [Pei et al., 2021](#); [Zieliński et al., 2025](#)) employed 2D DIC, which struggles with out-of-plane motions and decorrelation at crack tips. Stereo (3D) systems ([Cheng et al., 2022](#); [Jiang-san et al., 2022](#); [Kong et al., 2023](#); [Wang et al., 2020](#)) improve accuracy but add complexity, cost, and calibration overhead, making them impractical for routine or field testing. Furthermore, studies like [Liang et al. \(2020\)](#) and [Radeef et al. \(2021\)](#) combined DIC with image processing (DIP) for crack length estimation, introducing indirect methods and additional post-processing steps that increase computational burden and reduce reproducibility. Finally, reporting gaps and reproducibility concerns persist. Several papers ([Pei et al., 2021](#); [Zhang et al., 2018](#); [Zieliński et al., 2025](#)) omit key imaging parameters such as resolution, frame rate, and calibration details, hindering benchmarking and standardization. [Pei et al. \(2021\)](#) explored natural surface textures to avoid speckle preparation, but robustness under varying lighting and aggregate heterogeneity remains uncertain.

### **3. EXPERIMENTAL FRAMEWORK**

To ensure a coherent experimental workflow, the preparation of specimens and their subsequent SCB testing form the foundation for reliable fracture performance evaluation. Building on these physical tests, an advanced imaging strategy is integrated to capture and analyse crack propagation and deformation patterns in detail. This transition from mechanical testing to feature-based tracking enables a comprehensive understanding of material behaviour under loading, bridging traditional laboratory methods with digital analysis.

### ***3.1. Specimen preparation and SCB testing***

Building on the detailed methodology reported by [Abut \(2024\)](#), this study ensured consistency in specimen preparation and SCB test reliability. Cylindrical specimens ( $\Phi 150 \text{ mm} \times 50 \text{ mm}$ ) were fabricated following the Marshall procedure and [EN \(2022\)](#) standards to ensure uniformity in mixture design and compaction. Each specimen was compacted in Proctor moulds ( $\Phi 150 \times 116.4 \text{ mm}$ ) using a vibrating hammer (BOSCH GBH 11 DE, 11 kg, 900 W, 2000 impacts/min) at  $135^\circ\text{C}$ . Compaction time was optimized through trial and error, and acceptance criteria required  $\geq 98\%$  of the target unit weight and air voids near 4%. Specimens failing these conditions were excluded. After curing for 24 hours, discs were demoulded and cut into semi-circular halves using a precision disc saw. A notch was introduced at the mid-span to create the ligament necessary for fracture testing. In accordance with [AASHTO \(2020a\)](#), specimens were conditioned at  $-12^\circ\text{C}$  for  $2 \pm 0.5$  hours prior to testing. Monotonic bending tests were performed using an INSTRON 5982 universal testing machine (capacity: 100 kN; sensitivity: 0.16%). Crack Mouth Opening Displacement (CMOD) was monitored with a gauge (range: 0–4 mm; resolution: 0.003 mm), synchronized with load acquisition at 10 Hz. The system is capable of recording CMOD and load data at intervals of one-tenth of a second, ensuring high temporal resolution for correlating mechanical response with crack evolution. The loading rate was maintained at 0.5 mm/min to ensure quasi-static conditions. Fracture parameters—work of fracture, fracture energy, fracture toughness, and stiffness—were calculated according to [AASHTO \(2020a\)](#) to characterize crack initiation and propagation under tensile-dominated conditions.

### ***3.2. Imaging Strategy for the Feature-Based Tracking***

To capture crack evolution during SCB tests, a low-cost imaging approach was implemented using a webcam (Logitech HD Pro C910). Images were recorded every 5 seconds at  $2304 \times 1536 \text{ px}$  ( $\approx 3.5 \text{ MP}$ , 96 dpi, bit depth: 8) without additional lighting or artificial speckle patterns (Figure 1). To enhance surface visibility, a thin layer ( $\sim 1\text{--}2 \text{ mm}$ ) was trimmed from the specimen face, exposing aggregate texture for natural feature tracking. After trimming, fine dust was removed using compressed air to ensure a clean surface. This minimalist setup contrasts sharply with conventional DIC systems that require high-speed cameras, controlled illumination, and speckle preparation.

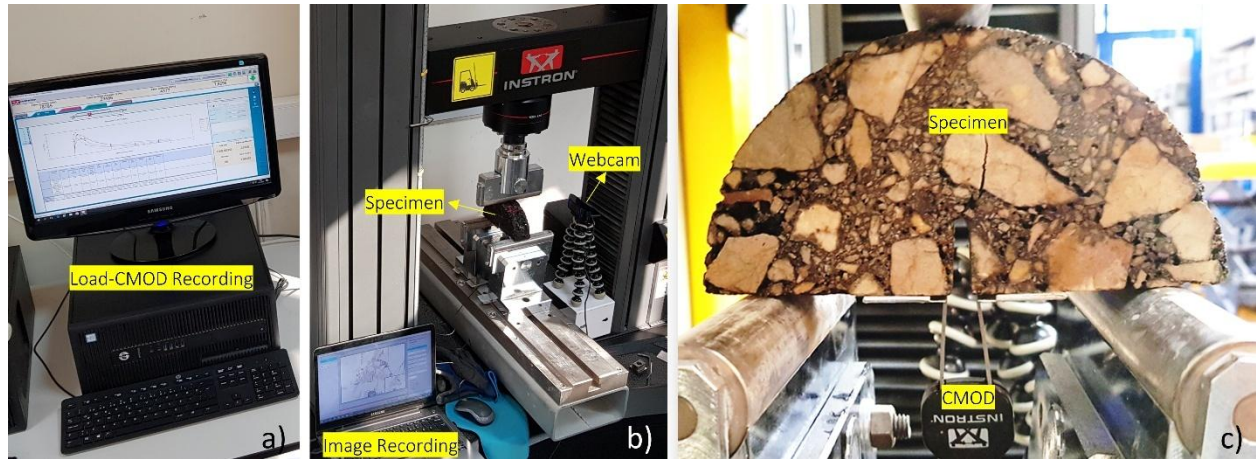


**Figure 1:** Experimental setup for SCB tests: (a) recording of load and CMOD during fracture test; (b) test frame, specimen, and low-cost imaging system using a webcam; (c) specimen and CMOD

#### **4. EXTRACTION OF ROI AND FEATURE BASED DISPLACEMENT ANALYSIS**

The analysis began with a targeted pre-processing stage to isolate the ROI surrounding the crack mouth and suppress background motion. Using manual annotation, a binary mask was generated on the reference image and then applied to the subsequent frame so that both images contained an identical, tightly bounded ROI. The masked images were converted to grayscale to normalize intensity and reduce computational load, yielding consistent inputs for feature detection (Figure 2).

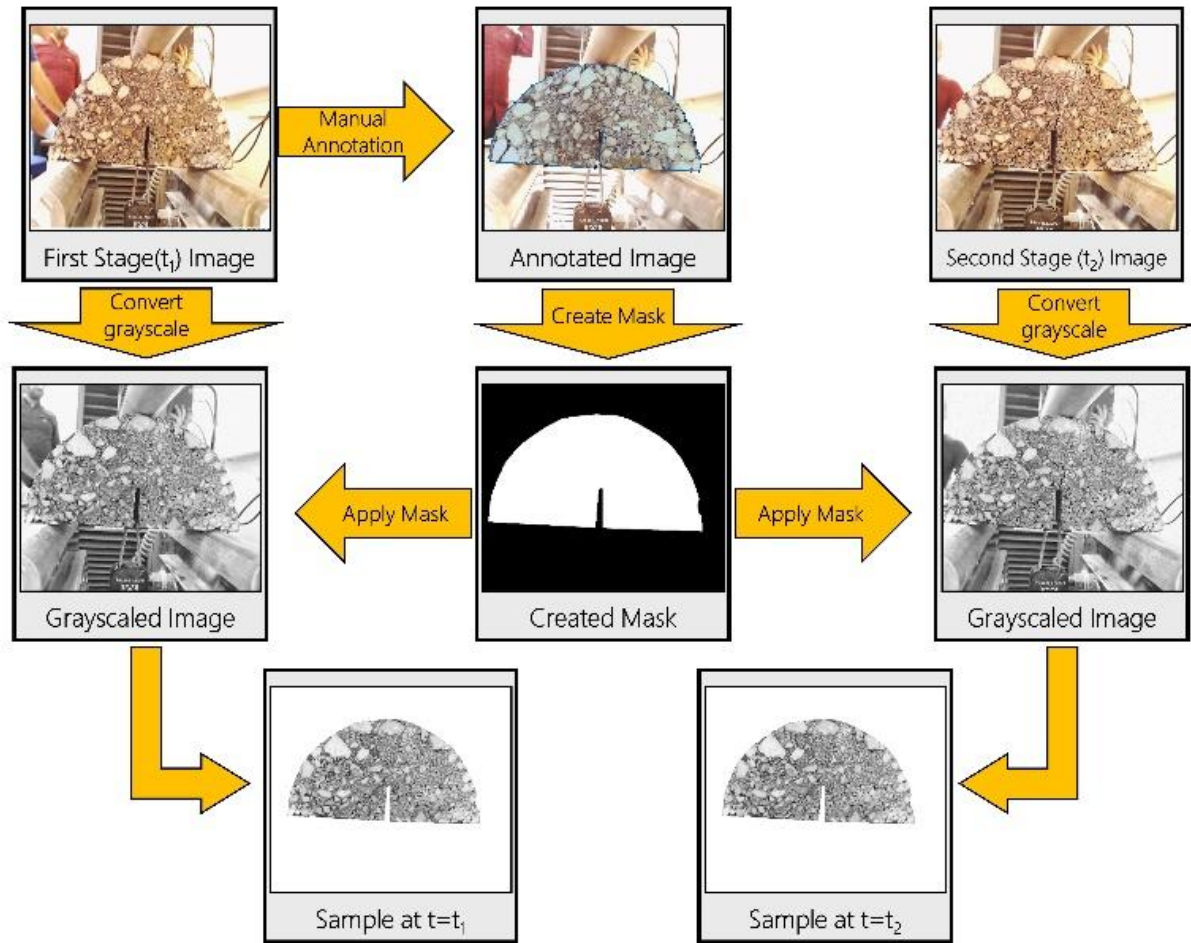


**Figure 2:** ROI definition workflow.

Within the ROI, landmark points were detected using SURF, which is well suited to the heterogeneous, high contrast textures of asphalt mixtures (aggregate boundaries, binder matrix, and fine surface relief). The detector produced thousands of landmark points in a typical frame (e.g., 5,786 in the example shown), each encoded by a 64-element descriptor that captures the local neighbourhood structure around the feature (Figures 3–4). These descriptors provide invariance to modest geometric and photometric changes—an essential property given our low-cost imaging (webcam) and the absence of controlled illumination or artificial speckle.

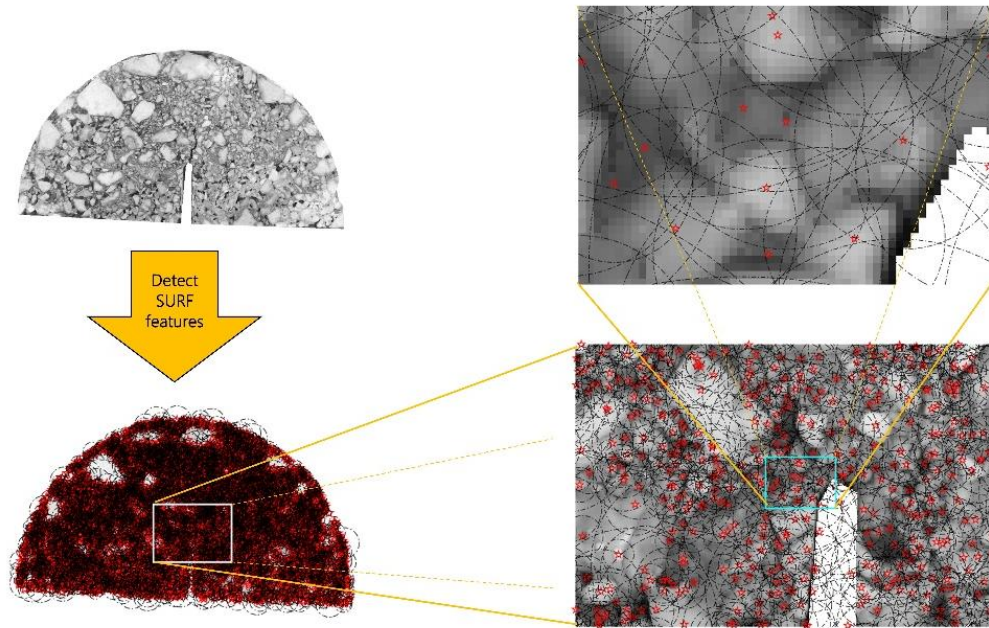


Figure 3: SURF landmark points (single frame).

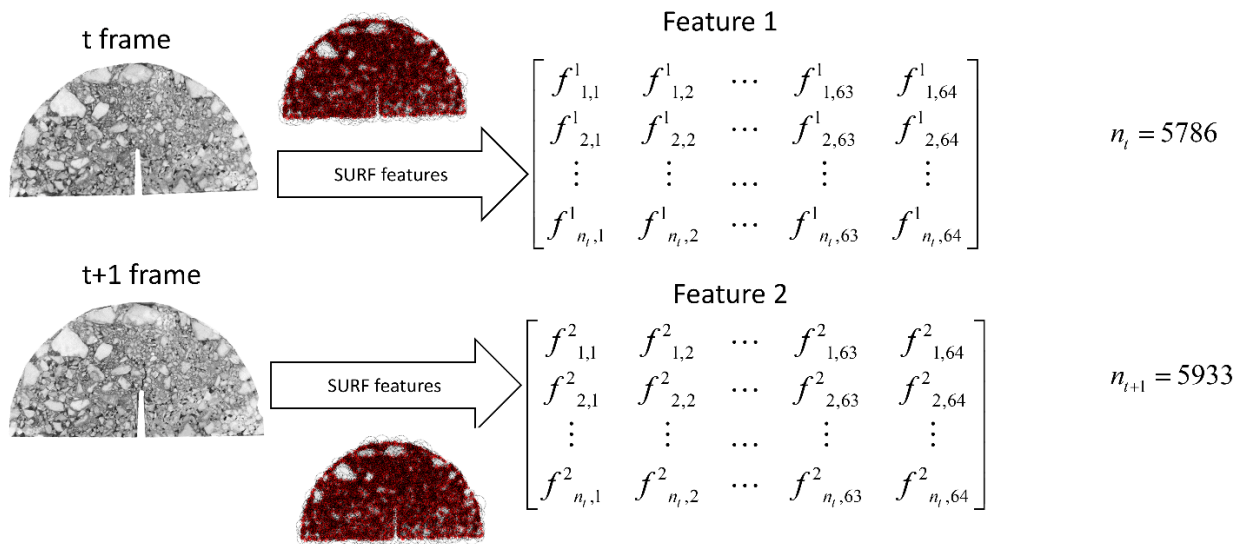


Figure 4: Descriptor inventory

To estimate motion between frames, descriptors were paired using Sum of Absolute Differences (SAD). Matches with  $SAD < 0.6$  were retained while others were rejected, providing an initial, sparse displacement graph across the ROI (Figure 5). This thresholding step efficiently removed many ambiguous correspondences without the heavy iterative outlier suppression often required in correlation based DIC, aligning with the lightweight philosophy of our RiFT pipeline.

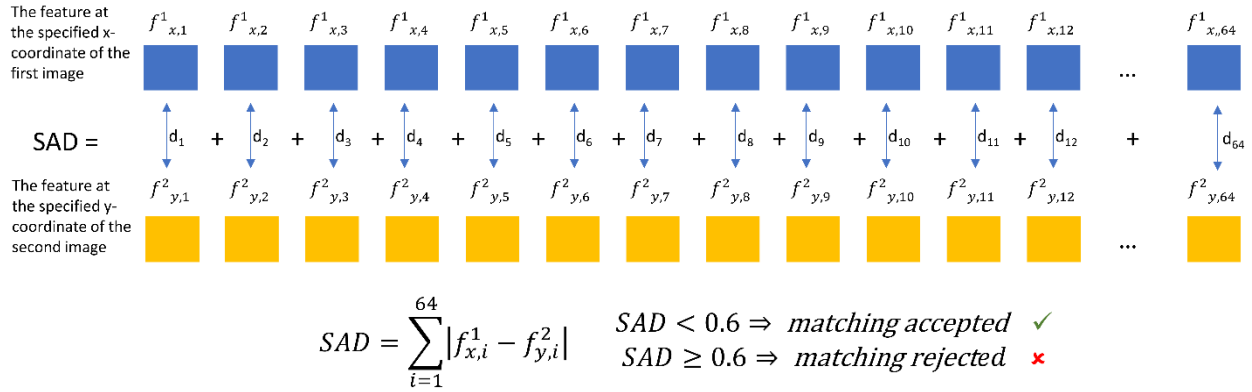


Figure 5: Inter frame matching ( $t \rightarrow t + 1$ ).

Residual spurious vectors were then filtered statistically. The empirical distribution of displacement magnitudes was computed, and vectors beyond the 95th percentile were discarded; these typically correspond to mismatches on weak texture patches or minor background contamination.

The effect is visible in the histogram guided culling and the cleaned vector field: the remaining tracks cluster along physically plausible deformation paths (Figure 6). This percentile-based rule adapts automatically to each image pair and avoids hand tuning for different mixtures or lighting conditions.

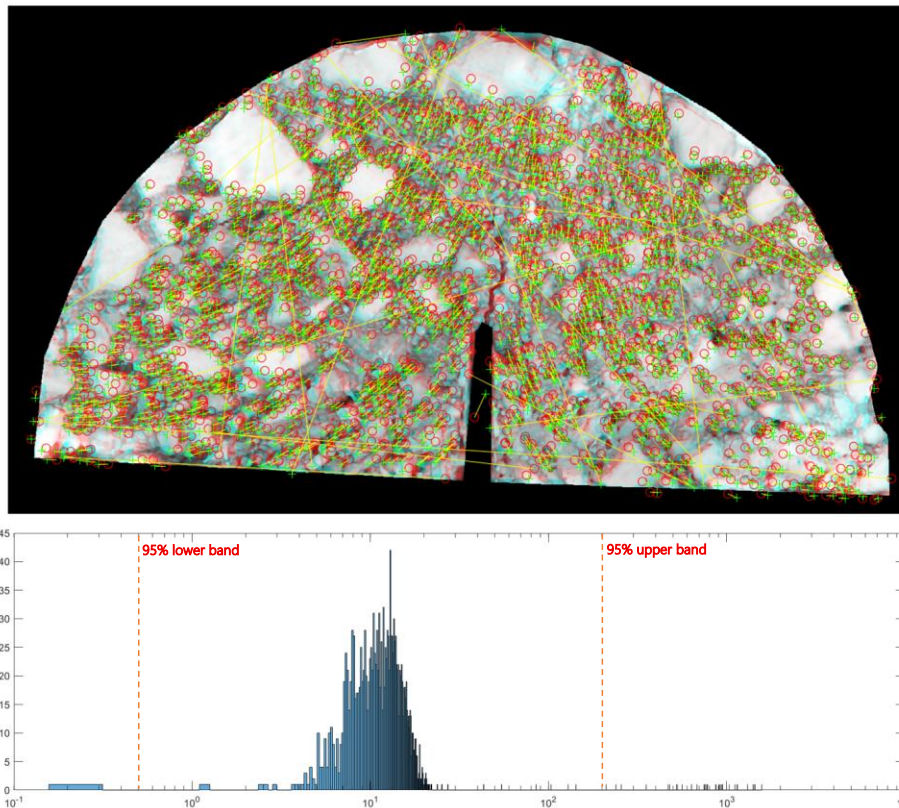
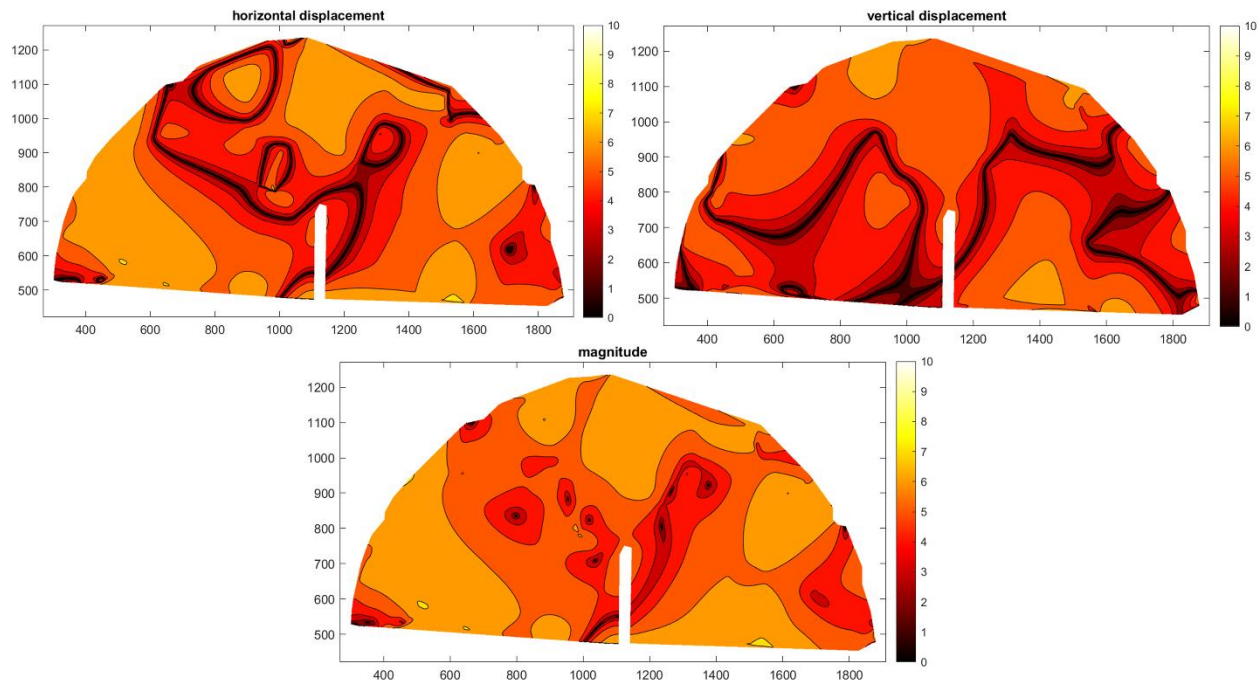


Figure 6: Outlier rejection.

The robust but sparse motion samples were interpolated to a dense displacement field using an edge aware scheme that respects crack driven discontinuities. The resulting component maps horizontal displacement ( $U_x$ ), vertical displacement ( $U_y$ ) and the magnitude field reveal a clear localization of deformation in the ligament region adjacent to the notch, with gradients intensifying as the crack mouth opens (Figure 7). All three contour maps utilize two-unit systems: arbitrary position units ( $U_{pos}$ ) for the coordinates of landmark points and arbitrary displacement units ( $U_{disp}$ ) (on a 0-10 scale) for the displacements of the landmark points. While all plots confirm that the highest deformation is clearly localized to the ligament region compared to the rest of the specimen, a critical observation is that the maximum values ( $\approx 9-10 U_{disp}$ ) are not concentrated at a single point but are distributed across multiple interconnected centres. These distributed maxima in both the  $U_x$  and  $U_y$  maps suggest a non-uniform stress distribution within the material (likely due to its heterogeneous nature) and indicate that the Fracture Process Zone (FPZ) develops as an area rather than a single crack line.  $U_x$  model the natural crack formation (opening) in the horizontal direction due to crack propagation, while  $U_y$  model the compression effect resulting from the loading applied by the support areas at the top and bottom points of the specimen. Consequently, the magnitude map confirms that this dispersed area peaks in total displacement, strongly demonstrating that the deformation within the ligament is localized yet simultaneously heterogeneous, occurring around multiple regions of micro-cracking.



**Figure 7:** Dense field maps.

Finally, crack evolution was visualized by overlaying the displacement magnitude on the ROI and inspecting successive frames. The concentration bands align with the visually observed fracture path and expand temporally in a manner consistent with the Load–CMOD response captured by the test machine; the final panel shows the mature crack trajectory within the ROI (Figure 2). Taken together, Figures 2–7 demonstrate that a SURF based, threshold and percentile filtered matching pipeline, followed by edge preserving interpolation, can recover sub pixel scale, spatially coherent motions with minimal hardware and pre-processing—capturing the onset and growth of cracking in SCB tests using standard webcam imagery.

## **5. CONCLUSION AND RECOMMENDATIONS**

This study introduced a feature-based displacement tracking framework, RiFT, as an alternative to conventional correlation-heavy methods such as DIC for monitoring crack evolution in asphalt mixtures under SCB loading.

These advantages position RiFT as a scalable solution for fracture analysis in asphalt pavements and other quasi-rigid materials, particularly where resource constraints or field conditions limit the feasibility of conventional DIC systems, thus maximizing the utility of the standard SCB test.

The experimental results demonstrated that RiFT can accurately capture sub-pixel displacements and visualize crack propagation using standard-resolution images acquired from a webcam, without the need for speckle patterns, controlled lighting, or high-speed acquisition systems. By leveraging SURF-based landmark point detection and robust matching combined with percentile-based outlier filtering and edge-preserving interpolation, RiFT achieved reliable displacement fields while significantly reducing computational complexity and hardware costs.

While this study successfully validates the RiFT framework under controlled laboratory conditions using a single asphalt mixture type, future research is necessary to fully benchmark its accuracy across different mixtures and to validate its robustness under diverse field lighting and texture conditions (See Section 6).

The findings confirm that RiFT addresses key limitations of traditional optical methods:

- Eliminates dependency on expensive cameras and elaborate calibration procedures.
- Maintains accuracy under modest angular and illumination variations, making it suitable for field conditions.
- Sparse feature matching and interpolation reduce processing time compared to full-field correlation approaches.

These advantages position RiFT as a scalable solution for fracture analysis in asphalt pavements and other quasi-rigid materials, particularly where resource constraints or field conditions limit the feasibility of conventional DIC systems.

## **6. RECOMMENDATIONS FOR FUTURE WORK**

- Extend RiFT to fatigue SCB tests and cyclic loading scenarios, where crack evolution occurs over thousands of cycles.
- Explore feature selection and displacement prediction using deep learning to further improve robustness under noisy conditions.
- Validate RiFT in real pavement sections under in-service conditions, assessing its adaptability to uncontrolled lighting and environmental variability.
- Benchmark RiFT against DIC-based fracture indicators (e.g., J-integral, flexibility index) to establish conversion relationships for design standards.
- Incorporate automated segmentation techniques to eliminate manual annotation, enabling fully autonomous image processing pipelines.

By addressing these directions, RiFT can evolve into a comprehensive, low-cost, and field-ready tool for structural health monitoring and pavement performance evaluation.

## **CONFLICT OF INTEREST STATEMENT**

There is no conflict of interest among the authors.

## **ACKNOWLEDGEMENT**

The author of this article would like to gratefully acknowledge KORDSA Teknik Tekstil A.Ş. for the fracture tests of SCB specimens into the experimental works.

## **CONTRIBUTIONS OF AUTHORS**

Y.A.: Conceptualization, methodology, software, validation, formal analysis, investigation, resources, writing, review and editing —original draft preparation

## **REFERENCES**

- AASHTO. (2014). *AASHTO T322: Determining the Creep Compliance and Strength of Hot Mix Asphalt (HMA) Using the Indirect Tensile Test Device* AASHTO.
- AASHTO. (2017). *AASHTO T321: Standard Method of Test for Determining the Fatigue Life of Compacted Hot Mix Asphalt (HMA) Subjected to Repeated Flexural Bending*. In. Washington, DC: AASHTO.

- AASHTO. (2020a). *AASHTO TP 105: Standard Method of Test for Determining the Fracture Energy of Asphalt Mixtures Using the Semicircular Bend Geometry (SCB)*. American Association of State Highway and Transportation Officials (AASHTO).
- AASHTO. (2020b). *AASHTO TP 124: Standard Method of Test for Determining the Fracture Potential of Asphalt Mixtures Using the Illinois Flexibility Index Test (I-FIT)*. American Association of State Highway and Transportation Officials (AASHTO).
- Abut, Y. (2024). Experimental Investigation of the Fracture Properties for Crumb Rubber Modified (CRM) Asphalt Mixtures [Granül Kauçuk Modifiyeli (CRM) Asfalt Karışımların Kırılma Özelliklerinin Deneysel Olarak İncelenmesi]. *Politeknik Dergisi*, 27(2), 515-522. <https://doi.org/10.2339/politeknik.1125034>
- Alsheyab, M. A., Khasawneh, M. A., Abualia, A., & Sawalha, A. (2024). A critical review of fatigue cracking in asphalt concrete pavement: a challenge to pavement durability. *Innovative Infrastructure Solutions*, 9(10), 386. <https://doi.org/10.1007/s41062-024-01704-1>
- Asswad, J., Ziade, E., Tehrani, F. F., & Pop, I. O. (2024). Assessment of resistance to crack propagation of asphalt mixtures using two parts digital image correlation. *Theoretical and Applied Fracture Mechanics*, 133, 104578. <https://doi.org/https://doi.org/10.1016/j.tafmec.2024.104578>
- ASTM. (2013). *ASTM D7313: Standard Test Method for Determining Fracture Energy of Asphalt Mixtures Using the Disk-Shaped Compact Tension Geometry*. ASTM International.
- ASTM. (2016). *ASTM D8044: Standard Test Method for Evaluation of Asphalt Mixture Cracking Resistance using the Semi-Circular Bend Test (SCB) at Intermediate Temperatures*. ASTM International.
- ASTM. (2017). *ASTM D6931: Standard Test Method for Indirect Tensile (IDT) Strength of Asphalt Mixtures*. ASTM International.
- ASTM. (2021). *ASTM D8237: Standard Test Method for Determining Fatigue Failure of Asphalt-Aggregate Mixtures with the Four-Point Beam Fatigue Device*. ASTM International. <https://doi.org/10.1520/D8237-21>
- Bay, H., Tuytelaars, T., & Van Gool, L. (2006, 2006/). SURF: Speeded Up Robust Features. Computer Vision – ECCV 2006, Berlin, Heidelberg.
- Birgisson, B., Montepara, A., Romeo, E., Roncella, R., Napier, J. A. L., & Tebaldi, G. (2008). Determination and prediction of crack patterns in hot mix asphalt (HMA) mixtures. *Engineering Fracture Mechanics*, 75(3), 664-673. <https://doi.org/https://doi.org/10.1016/j.engfracmech.2007.02.003>
- Cabo, C., Ordóñez, C., Muñoz-Calvente, M., Lozano, M., & Ismael, G. (2019). A hybrid SURF-DIC algorithm to estimate local displacements in structures using low-cost conventional cameras. *Engineering Failure Analysis*, 104, 807-815. <https://doi.org/https://doi.org/10.1016/j.engfailanal.2019.06.083>
- Cheng, L., Zhang, L., Liu, X., Yuan, F., Ma, Y., & Sun, Y. (2022). Evaluation of the fatigue properties for the long-term service asphalt pavement using the semi-circular bending tests and stereo digital image correlation technique. *Construction and Building Materials*, 317, 126119. <https://doi.org/https://doi.org/10.1016/j.conbuildmat.2021.126119>
- EN. (2010). *EN 12697-44: Bituminous mixtures – Test methods – Part 44: Crack propagation by semi-circular bending test*. European Committee for Standardization (CEN). <https://www.en-standard.eu/din-en-12697-44-bituminous-mixtures-test-methods-part-44-crack-propagation-by-semi-circular-bending-test/>
- EN. (2022). *EN 12697-32: Bituminous Mixtures, Test Methods for Hot Mix Asphalt, Laboratory Compaction of Bituminous Mixtures by Vibratory Compactor*. European Committee for Standardization (CEN). <https://www.en-standard.eu/csn-en-12697-32-bituminous-mixtures-test-methods-part-32-specimen-preparation-by-vibratory-compactor/>
- Górszczyk, J., Malicki, K., & Zych, T. (2019). Application of Digital Image Correlation (DIC) Method for Road Material Testing. *Materials*, 12(15). <https://doi.org/10.3390/ma12152349>
- Hassan, M. M. (2013). Effect of secondary aggregates on relationship between creep time dependent index and Paris Law parameters. *Journal of Civil Engineering and Construction Technology*, 4(2), 45-50. <https://doi.org/https://doi.org/10.5897/JCECT12.040>

- Huang, B., Shu, X., & Zuo, G. (2013). Using notched semi circular bending fatigue test to characterize fracture resistance of asphalt mixtures. *Engineering Fracture Mechanics*, 109, 78-88. <https://doi.org/https://doi.org/10.1016/j.engfracmech.2013.07.003>
- Jiang-san, H., Lan, W., & Xin, L. (2022). Anti-fatigue performance of warm-mixed rubber powder modified asphalt mixture based on the DIC technique. *Construction and Building Materials*, 335, 127489. <https://doi.org/https://doi.org/10.1016/j.conbuildmat.2022.127489>
- Kong, L., Ren, D., Zhou, S., He, Z., Ai, C., & Yan, C. (2023). Evaluating the evolution of fiber-reinforced emulsified asphalt cold-recycled mixture damage using digital image correlation. *International Journal of Pavement Engineering*, 24(1), 2176495. <https://doi.org/10.1080/10298436.2023.2176495>
- Li, X. J., & Marasteanu, M. O. (2010). Using Semi Circular Bending Test to Evaluate Low Temperature Fracture Resistance for Asphalt Concrete. *Experimental Mechanics*, 50(7), 867-876. <https://doi.org/10.1007/s11340-009-9303-0>
- Liang, H., Wang, D., Shi, L., Liang, X., & Tang, C. (2020). Use of digital images for fracture performance evaluation of asphalt mixtures. *Construction and Building Materials*, 253, 119152. <https://doi.org/https://doi.org/10.1016/j.conbuildmat.2020.119152>
- Lu, D. X., Bui, H. H., & Saleh, M. (2021). Effects of specimen size and loading conditions on the fracture behaviour of asphalt concretes in the SCB test. *Engineering Fracture Mechanics*, 242, 107452. <https://doi.org/https://doi.org/10.1016/j.engfracmech.2020.107452>
- Ma, Y., Mohammad, L. N., Liu, J., Asghar, M., Elnaml, I., Cooper, S. B., & Cooper, S. B. (2024). Development of a cyclic semi-circular bending test protocol to characterize fatigue cracking of asphalt mixture at intermediate temperature. *Construction and Building Materials*, 443, 137669. <https://doi.org/https://doi.org/10.1016/j.conbuildmat.2024.137669>
- Marasteanu, M., Buttlar, W., Bahia, H., Williams, C., Moon, K. H., Teshale, E. Z., Falchetto, A. C., Turos, M., Dave, E., & Paulino, G. (2012). *Investigation of low temperature cracking in asphalt pavements national pooled fund study-phase II*.
- Min, W., Lu, P., Liu, S., & Wang, H. (2025). A Review of Crack Sealing Technologies for Asphalt Pavement: Materials, Failure Mechanisms, and Detection Methods. *Coatings*, 15(7). <https://doi.org/10.3390/coatings15070836>
- Ouyang, J., Yang, W., Cao, P., & Han, B. (2023). The fracture behaviour of cement bitumen emulsion mixture through the digital image correlation (DIC) method. *International Journal of Pavement Engineering*, 24(1), 2220065. <https://doi.org/10.1080/10298436.2023.2220065>
- Pei, Z., Lou, K., Kong, H., Wu, B., Wu, X., Xiao, P., & Qi, Y. (2021). Effects of Fiber Diameter on Crack Resistance of Asphalt Mixtures Reinforced by Basalt Fibers Based on Digital Image Correlation Technology. *Materials*, 14(23). <https://doi.org/10.3390/ma14237426>
- Radeef, H. R., Abdul Hassan, N., Mahmud, M. Z. H., Zainal Abidin, A. R., Ismail, C. R., Abbas, H. F., & Al-Saffar, Z. H. (2021). Characterisation of cracking resistance in modified hot mix asphalt under repeated loading using digital image analysis. *Theoretical and Applied Fracture Mechanics*, 116, 103130. <https://doi.org/https://doi.org/10.1016/j.tafmec.2021.103130>
- Saha, G., & Biligiri, K. P. (2015). Fracture damage evaluation of asphalt mixtures using Semi-Circular Bending test based on fracture energy approach. *Engineering Fracture Mechanics*, 142, 154-169. <https://doi.org/https://doi.org/10.1016/j.engfracmech.2015.06.009>
- Saha, G., & Biligiri, K. P. (2016). Fracture properties of asphalt mixtures using semi-circular bending test: A state-of-the-art review and future research. *Construction and Building Materials*, 105, 103-112. <https://doi.org/https://doi.org/10.1016/j.conbuildmat.2015.12.046>
- Son, S. (2014). *Development of a Phenomenological Constitutive Model for Fracture Resistance Degradation of Asphalt Concrete with Damage Growth Due to Repeated Loading* [Dissertation, University of Illinois at Urbana-Champaign]. Urbana, Illinois. <https://www.ideals.illinois.edu/items/49876>
- Texas. (2025). *Tex-248-F: Test procedure for the overlay test*. Texas Department of Transportation (TxDOT).

- Wang, L., Shan, M., & Li, C. (2020). The cracking characteristics of the polymer-modified asphalt mixture before and after aging based on the digital image correlation technology. *Construction and Building Materials*, 260, 119802. <https://doi.org/https://doi.org/10.1016/j.conbuildmat.2020.119802>
- Zhang, J., Sakhaeifar, M., Little Dallas, N., Bhasin, A., & Kim, Y.-R. (2018). Characterization of Crack Growth Rate of Sulfur-Extended Asphalt Mixtures Using Cyclic Semicircular Bending Test. *Journal of Materials in Civil Engineering*, 30(12), 04018311. [https://doi.org/10.1061/\(ASCE\)MT.1943-5533.0002517](https://doi.org/10.1061/(ASCE)MT.1943-5533.0002517)
- Zhao, Y., Ni, F., Zhou, L., & Jiang, J. (2017). Heterogeneous fracture simulation of asphalt mixture under SCB test with cohesive crack model. *Road Materials and Pavement Design*, 18(6), 1411-1422. <https://doi.org/10.1080/14680629.2016.1230071>
- Zhou, F., Newcomb, D., Gurganus, C., Banihashemrad, S., Park, E. S., Sakhaeifar, M., & Lytton, R. L. (2016). *Experimental design for field validation of laboratory tests to assess cracking resistance of asphalt mixtures* (NCHRP Project, Issue. [https://onlinepubs.trb.org/onlinepubs/nchrp/docs/NCHRP09-57\\_FR.pdf](https://onlinepubs.trb.org/onlinepubs/nchrp/docs/NCHRP09-57_FR.pdf)
- Zieliński, P., Klimczak, M., Tekieli, M., & Strzpek, M. (2025). An Evaluation of the Fracture Properties of Asphalt Concrete Mixes Using the Semi-Circular Bending Method and Digital Image Correlation. *Materials*, 18(5). <https://doi.org/10.3390/ma18050967>